JOC The Journal of Organic Chemistry

Article

Reaction cycling for kinetic analysis in flow

Ryan J Sullivan, and Stephen G. Newman

J. Org. Chem., **Just Accepted Manuscript** • DOI: 10.1021/acs.joc.0c00216 • Publication Date (Web): 23 Mar 2020

Reaction cycling for kinetic analysis in flow

Ryan J. Sullivan and Stephen G. Newman*

Centre for Catalysis Research and Innovation, Department of Chemistry and Biomolecular Sciences, University of Ottawa, 10 Marie-Curie, Ottawa, Ontario, Canada, K1N 6N5.

ABSTRACT: A reactor capable of efficiently collecting kinetic data in flow is presented. Conversion over time data is obtained by cycling a discrete reaction slug back-and-forth between two residence coils, with analysis performed each time the solution is passed between the two. In contrast to a traditional steady state continuous flow system, which requires upwards of 5 × the total reaction time to obtain reaction progress data, this design achieves much higher efficiency by collecting all data during a single reaction. In combination with minimal material consumption (reactions performed in 300 μL slugs), this represents an improvement in efficiency for typical kinetic experimentation in batch as well. Application to kinetic analysis of a wide variety of transformations (acylation, S_NAr, silylation, solvolysis, Pd catalyzed C–S cross-coupling and cycloadditions) is demonstrated, highlighting both the versatility of the reactor and the benefits of performing kinetic analysis as a routine part of reaction optimization/development. Extension to the monitoring of multiple reactions simultaneously is also realized by operating the reactor with multiple reaction slugs at the same time.

INTRODUCTION

Measuring reaction kinetics is a powerful tool for enabling optimization, mechanistic investigation, and scale-up.[1] Despite this, collection of kinetic data is often overlooked in lieu of less rigorous methods due to the laborious experimentation required. Recent advances in hardware, such as sampling tools and programmable liquid handling robotics, have sought to alleviate this problem.[2] Mathematically simpler approaches to analyzing data, such as the visual variable time normalization method, have also been successful in reducing the barrier to studying kinetics in routine applications.[3]

Continuous flow systems offer numerous advantages over batch systems such as ease of automation, incorporation of online analytics, efficient mixing, and access to a larger range of temperatures and pressures.[4] Knowledge of the reaction kinetics is crucial for optimizing residence time and reagent concentration to maximize throughput. However, acquiring kinetic data is often considered an area where batch reactors are superior due to convenient sampling over time (Figure 1A).[5] In contrast, time and space are coupled in a typical flow reactor, where a reaction's residence time is a function of the flow rate and distance travelled. Sampling over time must thus be carried out as a sequence of experiments with varied flow rate (Figure 1B).[6] While effective, this approach is wasteful of both time and materials. To highlight this disadvantage, Blackmond and co-workers monitored the progress of an aldol reaction that required 40 minutes to reach completion.[5] Due to the need to adjust flow rates and wait for steady state before collection of each data point, a 5-fold increase in total reaction time and material consumption was required for flow compared to batch.

Solutions to this problem have so far focused on using stepped or gradient flow rates and model fitting software to circumvent the need to collect steady-state samples.[7] However these are limited by the complicated mathematics required, and applications have thus far been restricted to relatively simple reactions. Furthermore, these methods sometimes suffer from an inability to unambiguously discriminate between potential reaction mechanisms without relying on chemical intuition.

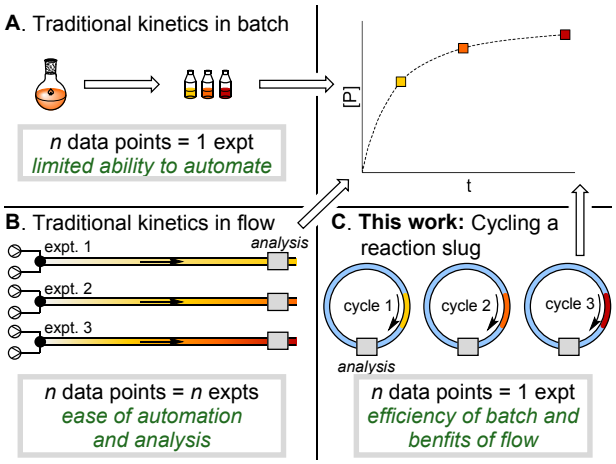

Figure 1. (A) Generation of reaction profiles in batch is accomplished by aliquot sampling over time. (B) Generation of reaction profiles in flow is accomplished by running a new steady-state experiment for each data point. (C) This work: A flow reactor capable of analyzing progress over time by cycling a reaction slug.

Given the growing number, diversity, and utility of advanced flow systems[8] and the expanding scope of reactions that can be performed equally well or better when run in flow,[9] we believed development of a simple and reliable method to obtain kinetic data from continuous systems would be invaluable. Flow reactors have proven particularly useful in the automated recovery and recycling of reaction components such as catalysts or auxiliaries through the implementation of recycling loops.[10] With this inspiration, we envisioned cycling an entire reaction solution by performing the reaction in discrete slugs[11] pushed by an inert, immiscible carrier fluid (Figure 1C). Analyzing the reaction once every loop provides reaction progress data.

Herein, we describe the design and implementation of such a reactor that enables straightforward acquisition of kinetic data. The versatility of this system is demonstrated through the study of a range of reaction types using varied solvents, temperatures, and kinetic analysis methods. The value of routinely performing kinetic analysis is additionally highlighted in the observation of non-intuitive rate behaviour for seemingly simple transformations. The setup is assembled from commercially available components, and data quality was comparable or superior to batch sampling. We thus believe that flow kinetics via reaction cycling will be useful for both routine analysis and as a component in more complex automation platforms. [12]

RESULTS AND DISCUSSION

Cycling a reaction slug through a reactor requires an inlet and outlet for the carrier stream to continuously enter and exit while somehow retaining the slug. In order to provide these essential features, we focused on developing a valve arrangement that facilitated cycling the slug along a looping figure eight path. This was accomplished by repurposing a commercially available 6-port, two-way injection valve and an 11-port, 10-position selector valve[13] by altering the fluid connectivity at the port connections and designing a custom rotor for the selector valve (see Figure S1 in the supporting information for full details). The modifications necessary are inexpensive[14] and easy to implement. The principle of operation is that when the reaction slug is in coil A it is directed to coil B and when in coil B it is directed back to coil A (Figure 2). Each time the slug is passed back and forth between the two reaction coils it travels through an intermediate zone where analysis is performed. While a range of online analysis tools can be envisioned,[15] we elected to use a sampling valve that removes a small aliquot for off-line analysis, keeping the system cost and complexity low.

While small droplets have been widely used as reaction slugs in automated screening and optimization platforms,[11] we used large slugs (>50 cm in length) to avoid problems with rate acceleration occurring at droplet/carrier stream interfaces[11a] and reaction solvent/reagent bleed/carryover into the carrier stream or subsequent slugs.[16] The immiscible carrier stream used can be either gaseous (e.g., N_2) or liquid (e.g., aqueous, fluorous, etc.) depending on the desired application; we demonstrate both options using N_2 and water respectively as carrier streams in different examples. The residence coils and remaining reactor materials can be selected for compatibility with the chemistry and conditions of interest; we opted for 0.5 mm ID PFA tubing for simplicity and optical transparency.

The ability to cycle slugs of solvent using the reactor was first examined. Solvent slugs with varying viscosity (H_2O, EtOH, toluene, $CHCl_3$) could be cycled using N_2 as the carrier stream without slug break up to provide a range of sampling intervals (~1.5–10 min between sample collections) over various temperatures (0–90 °C or ~5 °C below the atmospheric solvent boiling point of solvent). Above a certain limit, excessively high flow rates resulted in slug break up due to excessive shear forces with the reactor walls, but the accessible sampling intervals were more than sufficient to study the kinetics for the majority of reactions.[17] When using H_2O as the carrier stream, temperatures above solvent atmospheric boiling points could be used in combination with the application of system back pressure.

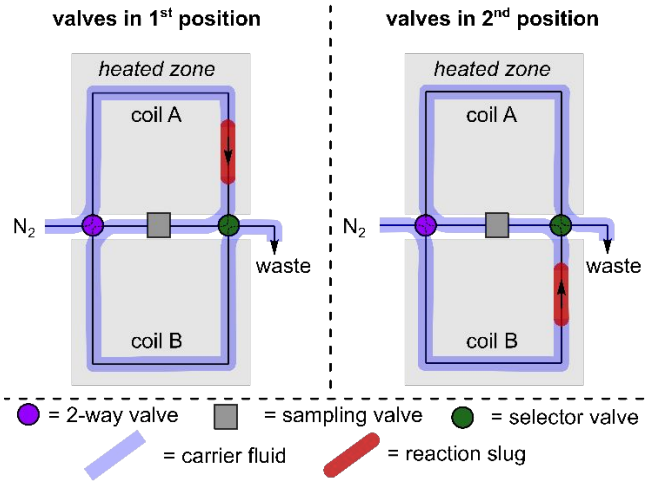

Figure 2. A schematic of the reactor coils and valves used to cycle a single reaction slug through a sampling valve multiple times, facilitating sequential sampling for reaction progress monitoring.

With the ability to cycle an inert slug confirmed, we next turned to the room-temperature acylation reaction between benzoyl chloride (**1**) and benzyl alcohol (**2**) as a well understood transformation to determine if reactions performed in the cycling flow reactor exhibited the same kinetic behaviour as under typical batch conditions. We selected Bu_3N (**3**) as the organic base to avoid solid handling issues,[9e] N_2 as the inert carrier stream to move the reaction slug[18] through the reactor, and the method of variable time normalization analysis (VTNA)[3] to analyze the data (Figure 3). In addition to performing experiments with the cycling flow reactor, all experiments were repeated using a traditional batch set-up (i.e., a round-bottom flask) for validation of the results obtained.

Identical results were observed in both cases, finding first order behaviour for both **1** (Figure 3A) and **2** (Figure 3B) and a partial reaction order of ~0.5 for **3** (Figure 3C). Related tertiary amine mediated acylation reactions are known to proceed by a nucleophilic catalysed mechanism,[19] and the positive reaction order observed for **3** agrees with this, although the partial order suggests a complex mechanism may be operative. By normalizing to all reaction components, a straight line is obtained with a slope equal to the rate constant (Figure 3D). Replication of experiments in batch showed indistinguishable kinetic profiles (e.g. Figure 3E) and found a value for the rate constant in excellent agreement with the value found using the cycling flow reactor (2% difference), confirming the validity and transferability of the collected data.

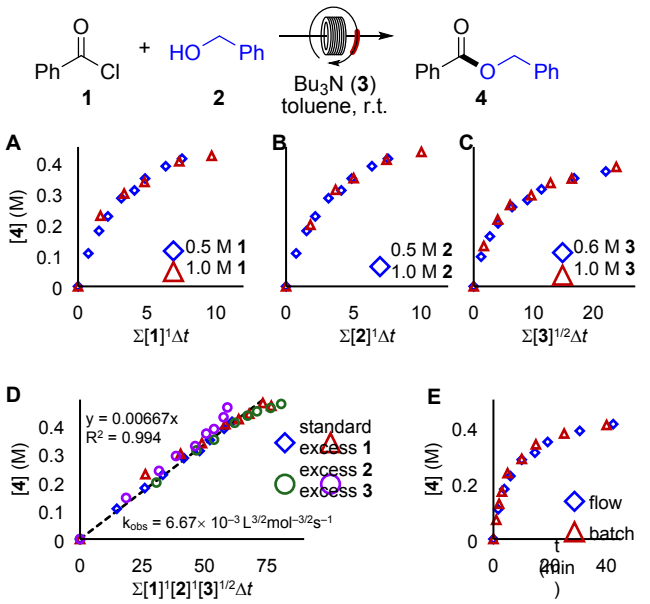

Figure 3. Kinetic data obtained using the cycling flow reactor. (A) VTNA plot showing 1st order in **1**. (B) VTNA plot showing 1st order in **2**. (C) VTNA plot showing ~0.5 order in **3**. (D) VTNA plot to calculate rate constant. (E) Overlay of data collected using flow reactor and batch data. Standard conditions: 0.5 M **1**, 0.5 M **2**, 0.6 M **3** in toluene, room temperature.

Satisfied that the reactor operated as desired, we next explored the ability to rapidly obtain kinetic data for a variety of reactions (Table 1). An S_NAr reaction at 80 °C (entry 1) and a silylation at 0 °C (entry 2) were examined to assess the reactor performance over a range of temperatures. The cycling flow reactor performed well in both cases, yielding identical reaction profiles with equivalent or slightly superior data quality (less noise) compared to parallel experiments in batch. The solvolysis of a secondary alkyl halide was probed using a pseudo-first order approach to distinguish between an S_N1 or S_N2 mechanism, as well as demonstrate the ability to perform an Eyring analysis by varying the reaction temperature (entry 3). A Pd catalysed C–S cross-coupling reaction was examined using the method of initial rates to show the applicability towards air- and moisture-sensitive chemistry and complex, multi-step reaction mechanisms (entry 4). Lastly, the ability to perform all necessary reactions simultaneously as consecutive slugs to maximize data collection efficiency was demonstrated with the analysis of a Diels-Alder cycloaddition (entry 5). The carrier fluid was also changed from N_2 to H_2O for this example to demonstrate the flexibility in choice of carrier solvent and the ability to conduct experiments above the atmospheric boiling point of the solvent ($CHCl_3$).

Table 1. Reactions investigated using the cycling flow reactor

Entry	Reaction	Analysis method	Demonstrating	Rate equation found
1	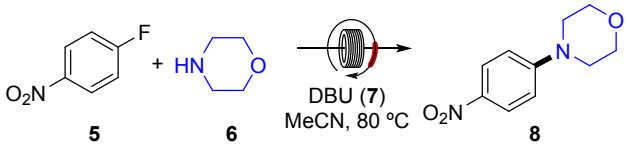	VTNA	Elevated temperature	rate = **[5][6]** 0th order in **7**
2	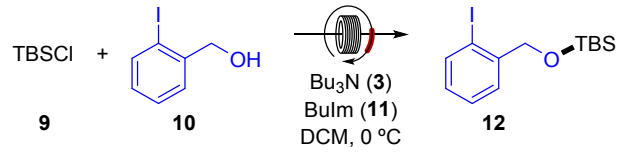	VTNA	Lowered temperature	rate = $\frac{k[9][10][11]^2}{[3]}$
3		pseudo-first order	Distinguish S_N1/S_N2; Temperature variation (Eyring analysis)	rate = k**[13][14]** 0th order in **15**
4	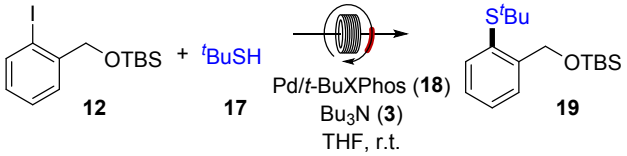	method of initial rates	O_2/H_2O free reaction; Complex mechanism	rate = k**[18][17]**^{x}**[3]**^{y} $0 < x,y < 1$ 0th order in **12** *saturation kinetics*
5	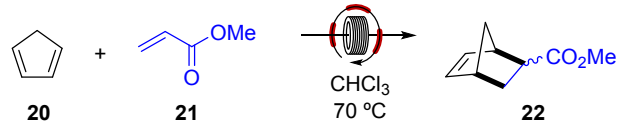	VTNA	Simultaneous reactions; Exceeding solvent b.p.; H_2O carrier phase	rate = **[20][21]**

The observed rate equation for the S_NAr reaction at elevated temperature was as expected, with first order behaviour observed for both electrophile **5** and nucleophile **6**, and 0th order for base **7**. Data obtained with the cycling flow reactor was in excellent agreement with the parallel data collected in batch, confirming that the choice of large slugs prevented appreciable loss of solvent to the gaseous carrier phase even when operating just below the atmospheric boiling point of the solvent. Investigating the silylation of alcohol **10** at lowered temperature provided further support that the kinetics obtained using the cycling flow reactor provide an accurate representation of the chemistry, with excellent agreement between the flow generated- and parallel batch generated-data.

In addition, a non-intuitive second order behaviour for the nucleophilic catalyst **11** and negative order with respect to base **3** were observed. This behavior contrasts with previous studies of the TBS protection of naphthalen-1-ylmethanol using DMAP or 1-methylimidazole as nucleophilic catalysts and Et_3N as the base.[20] In these cases first order in catalyst and no inhibitory effect of base was observed, highlighting the value of performing routine kinetic experiments even when changing substrates.

For the solvolysis of alkyl bromide **13**, selected to demonstrate the ability to distinguish between potential reaction mechanisms and determine activation parameters in flow, an S_N2 mechanism was found to be operative. First order behaviour for **13** was found using integrated rate laws under pseudo-first order conditions, to demonstrate the applicability of the reactor for other methods of kinetic analysis (Figure 4A). First order behaviour in EtOH (**14**) and zeroth order in acid **15** were determined by examining the effect of changing concentration on the observed rate constant (Table 2). Observing the effect of changing temperature on the rate constant allowed activation parameters to be calculated. An Eyring analysis of the data (Figure 4B, $k = k_{obs}/[EtOH]$) yielded values for the enthalpy (18.9 kcal/mol) and entropy (–15.2 cal/(mol·K)) of activation that were also consistent with an S_N2 mechanism.[21]

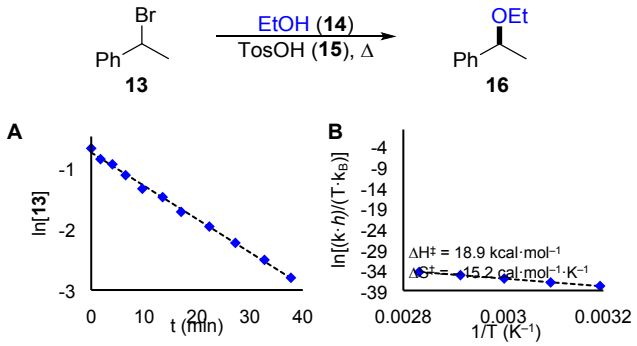

Figure 4. (A) Linear integrated rate law plot showing first order in electrophile **13.** (B) Eyring plot. Standard conditions: 0.5 M **13**, 0.125 M **15** in EtOH, 70 °C.

Table 2. k_{obs} values for the ethanolysis of 13.[a]

Entry	[**15**] (M)	[**14**] (M)	k_{obs}
1	0.125	16.0	0.0542
2	0.0250	16.0	0.0599
3	0.125	14.5[b]	0.0484
4	0.125	12.7[c]	0.0384

[a] All reactions 0.5 M in **13**. [b] 10:1 EtOH:*t*-BuOH as solvent. [c] 4:1 EtOH:*t*-BuOH as solvent.

To demonstrate the applicability of our reactor towards O_2 and H_2O sensitive chemistries and complex reaction mechanisms, a palladium catalysed C–S cross-coupling recently reported by Buchwald and co-workers was investigated.[22] First order behaviour was found for catalyst **18** (Figure 5A) and zeroth order for aryl halide **12** (Figure 5B), consistent with the previously identified $LPd^{II}ArX$ resting state,[22] by using the method of initial rates. The reaction orders for thiol **17** and base **3** proved to be more complex, yielding curving log-log plots of initial rate vs. concentration (Figure 5C and D). Both **17** and **3** exhibited saturation kinetics and Michaelis-Menten plots of the data fit well yielding v_{max} and K_M values for each reagent (Figure 5E and F). These data are consistent with a rate determining step of either deprotonation of the palladium bound thiol intermediate **III** or reductive elimination of the product from intermediate **IV** (see Figure 6). Subsequent DFT calculations concluded that reductive elimination is the rate limiting step (Figures S23–S25 in the supporting information). Not only was it possible to obtain high quality data for this air- and moisture-sensitive reaction using the cycling flow reactor, it was operationally simpler compared to the analogous batch experiment that would require sampling from a flask kept under inert atmosphere.

While experiments discussed thus far featured single reaction slugs cycled and analyzed over time, the ability to perform multiple reactions simultaneously, and therefore generate all data necessary for kinetic analysis at the same time, was envisioned. This is especially appealing for slow reactions, where the time required to collect all data is particularly tedious. The Diels-Alder reaction between cyclopentadiene (**20**) and methyl acrylate (**21**) required ~3 h to reach >80% conversion at 70 °C, making it an ideal candidate to demonstrate this ability. The volume of the residence coils was increased and the three necessary reactions (i.e., "standard conditions", and excess in each reagent) were injected as sequential slugs in a way that allowed the flow path to be altered each time all slugs were in the same residence coil (Figure 7).[23] The carrier phase was also changed from N_2 to water to allow the reaction to be conducted above the boiling point of the solvent through application of backpressure, highlighting another benefit of using a flow reactor over a batch setup.[24] In this way, all necessary data for kinetic analysis was collected in ~3 h, as opposed to the ~9 h that would have been required if running each reaction consecutively with this flow reactor, or the ~60 h that would be required to collect equivalent data using the traditional steady-state approach of changing the flow rate to change residence time for each data point.

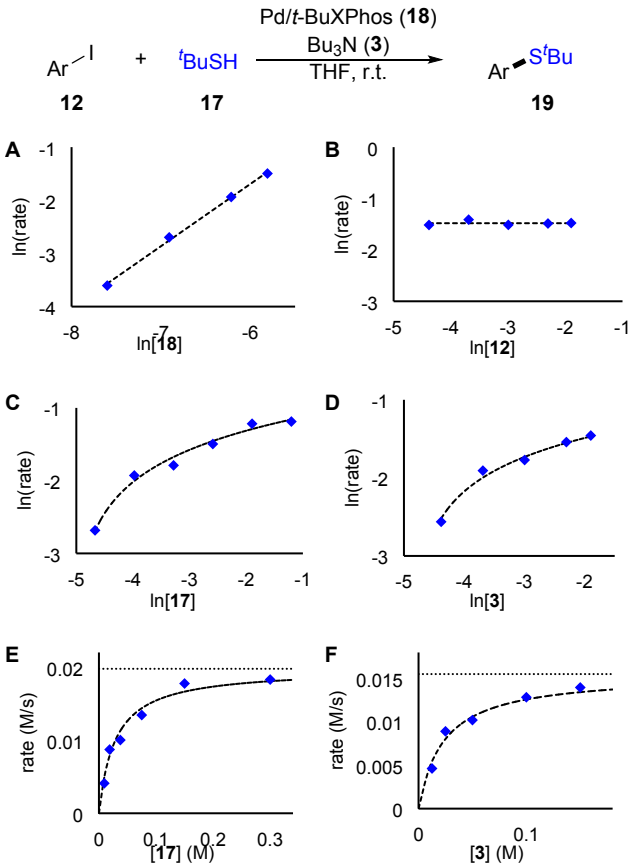

Figure 5. Initial rate kinetics for C–S cross coupling of ArI **12** and thiol **17** catalysed by a Pd/*t*-BuXPhos system. (A) log-log plot of initial rate vs. [**18**], (B) log-log plot of initial rate vs. [**12**], (C) log-log plot of initial rate vs. [**17**], (D) log-log plot of initial rate vs. [**3**], (E) Michaelis-Menten plot of initial rate vs. [**17**], (F) Michaelis-Menten plot of initial rate vs. [**3**]. Standard conditions: 50 mM **12**, 75 mM **17**, 100 mM **3**, 3 mM **18** in THF, room temperature.

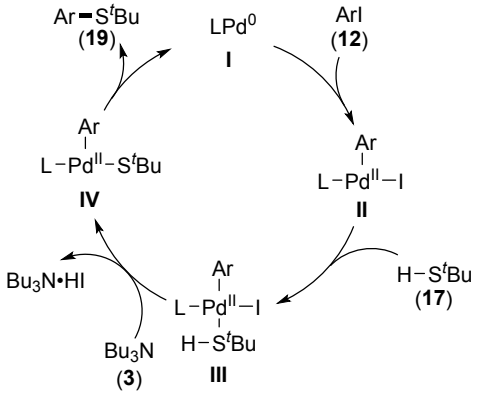

Figure 6. Putative catalytic cycle for the Pd catalysed C–S bond formation. L = *t*-BuXPhos, ArI = **12**.

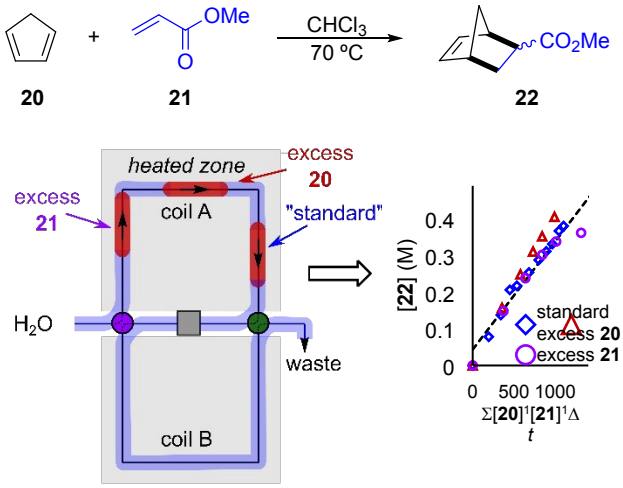

Figure 7. Operating with multiple sequential reaction slugs allows monitoring of multiple reactions simultaneously.

While the system has some limitations, in e.g., handling multi-phasic or extremely fast reactions, the ability to efficiently collect reaction progress data in flow, and applicability to a wide range of reactions and conditions holds promise for wide applicability.

CONCLUSION

We have developed a reactor that allows reaction progress to be monitored over time from a continuously cycling reaction slug. The reactor performance was assessed over a wide range of temperatures (0–80 °C), solvents (toluene, MeCN, DCM, EtOH, THF, $CHCl_3$) and reactions (acylation, S_NAr, silylation, ethanolysis, C–S cross-coupling, Diels-Alder). The ability to use the reactor to distinguish between potential reaction mechanisms and determine activation parameters was demonstrated. Lastly, the ability to perform multiple reactions simultaneously as consecutive reaction slugs was shown with the kinetic analysis of a Diels-Alder reaction.

The application of the reactor to collect data for a variety of different methods of kinetic analysis was also demonstrated, including variable time normalization analysis, pseudo-first order kinetics, Eyring plots and the method of initial rates. We believe the development of this reactor marks the first true equivalent in flow to the generation of reaction progress data in batch, where analysis over time from a single reaction solution is the most efficient strategy with regards to both time and material consumption. Therefore, since this reactor combines both the efficiency of the traditional batch sampling strategy with the benefits of flow, we believe this platform will lower the impediment to routine kinetic analysis, through both stand-alone operation and in combination with reaction platforms to automate kinetic experiments and data generation.

EXPERIMENTAL

General experimental details. Benzoyl chloride (**1**), benzyl alcohol (**2**), Bu_3N (**3**), TBSCl (**9**), cyclopentadiene (**20**) and methyl acrylate (**21**) were distilled before use. All other chemicals were obtained from commercial sources and used as received. THF was degassed with Ar and passed through a PureSolv solvent purification system before use. Solutions for

thiol cross-coupling reactions were prepared in oven-dried glassware under an Ar atmosphere.

NMR spectra were collected on a Bruker Avance 400 MHz spectrometer. ^{1}H and ^{13}C were referenced to residual solvent signals. GC yields for all kinetic studies were obtained via 5 or 6-point calibration curves using FID analysis on an Agilent Technologies 7890B GC with 30 m × 0.25 mm HP-5 column. For all reactions analyzed using VTNA or the method of initial rates the concentration of the product was determined by GC and the remaining reagent concentrations were calculated through mass balance assertion (i.e., stoichiometry). For the ethanolysis reaction the concentration of starting material (1-bromoethylbenzene) was monitored. For quantification of the C–S cross-coupling product **22**, the GC response factor (i.e., calibration curve slope) was determined by quantifying the disappearance of aryl iodide **12** and monitoring the appearance of the product peak for a reaction where conversion of **12** was taken to completion. For calculation of the unreacted cyclopentadiene concentration, both the methyl 5-norbornen-2-carboxylate product and the dicyclopentadiene by-product were quantified and taken into account.

Benzyl benzoate (4). To a solution of benzoyl chloride (0.56 g, 4.0 mmol) in toluene (5 mL) was added benzyl alcohol (0.47 g, 4.4 mmol) and Et_3N (0.44 g, 4.4 mmol) and stirred 15 min at 40 °C. The resulting suspension was then washed with 1 M HCl (5 mL) and the organic phase dried over Na_2SO_4. Evaporation of the solvent and purification on silica gel (25 × 100 mm, hexanes→5% EtOAc in hexanes eluent) yielded the pure product as a colourless oil. Yield 0.57 g (67%). Characterization data were in agreement with the literature.[25]

4-(4-Nitrophenyl)morpholine (8). The compound was prepared according to the literature procedure and characterization data were in agreement.[9e]

***tert*-Butyl((2-iodobenzyl)oxy)dimethylsilane (12)**. 2-Iodobenzyl alcohol (1.2 g, 5.1 mmol) and TBSCl (0.9 g, 6.0 mmol) were dissolved in 1-methylimidazole (5 mL, 63 mmol) and stirred 10 min at room temperature then 10 min at 35 °C. The solution was diluted with 50 mL 2:1 EtOAc:hexanes and washed with 15 mL 5 M HCl then 2 × 15 mL 1 M HCl and the organic phase dried over Na_2SO_4. The solvent was evaporated and the residue chromatographed on silica gel (25 × 100 mm, hexanes → 5% EtOAc in hexanes eluent) to yield the pure product as a colourless oil. Yield 1.60 g (90%). Characterization data were in agreement with the literature.[9e]

Methyl 5-norbornene-2-carboxylate (22). Cyclopentadiene (0.93 mL, 11 mmol) and methyl acrylate (0.90 mL, 10 mmol) were combined in $CHCl_3$ (20 mL) and refluxed 4 h. The solvent was evaporated and the residue chromatographed on silica gel to yield the pure product as a colourless oil in ~3:1 mixture of isomers. Characterization data were in agreement with the literature.[26]

Exemplary procedure: Benzoyl chloride + benzyl alcohol. *General procedure*. Solutions of **1** with hexadecane were prepared in toluene ("electrophile solutions"). Solutions of **2** with **3** were prepared in toluene ("nucleophile solutions"). For each reaction, 0.5 mL of desired electrophile solution and 0.5 mL of desired nucleophile solution were separately loaded into two 2.5 mL Hamilton glass syringes, installed onto the Chemxy fusion 200 dual channel syringe pump and primed, then connected cross-mixer of the flow reactor (see Figure S2 in the supporting information).

The N_2 flow was set to 3 mL/min for 2 min (to quickly establish pressure equilibration with the back pressure) then set to 0.8 mL/min. Valve 1 was set to position 1, valve 2 was set to position 1 (see Figure S1 in the supporting information) and the sampling valve was set to collect a sample. The 2-way valve was closed (to interrupt the N_2 flow) and 0.15 mL of each solution was dispensed by the syringe pump at a rate of 1.5 mL/min to form a 0.30 mL the reaction slug (~5 s). The 2-way valve was opened to let the reaction slug travel through coil A to valve 2 to the sampling valve.

Once ~50 µL of the slug passed through the sampling valve, the valve was actuated and a 15 µL aliquot sample was eluted with 600 µL EtOAc into a GC vial containing 100 µL MeOH to quench. Once the remainder of the reaction slug had exited the sampling valve and fully passed through valve 1 to coil B, valve 1 was set to position 2, valve 2 was set to position 2 (clockwise rotation) and the sampling valve was set to collect a sample again.

Notes: 1) Valve 1 is actuated before valve 2 to maintain N_2 pressure behind the reaction slug. If valves are actuated in reverse order, pressure is released behind the reaction slug causing interruptions to the flow. 2) The sampling valve is actuated at this time to empty the sample loop before the reaction slug returns to the valve and prevent contamination/dilution of the reaction slug with the solvent used to flush the sample loop by sending the contents of the sample loop through the other reactor coil to waste.

The reaction slug travelled through coil B, passing through valve 2 to the sampling valve. As with the first sample, once the first ~50 µL of the reaction slug had passed through the sampling valve it was actuated to collect the second sample which was quenched into a new GC vial in the same manner as the first sample. Again, after the reaction slug had fully passed though the sampling valve and valve 1, the valves were actuated: valve 1 to position 1, valve 2 to position 1 (counter-clockwise rotation), and the sampling valve to collect a new sample.

This sequence of sample collection + valve actuation was repeated to collect subsequent samples. To increase the time increment between samples, the flow rate of N_2 was decreased to 0.4 mL/min after the 3rd sample was collected and to 0.2 mL/min after the 6th sample was collected. This procedure allowed the collection of aliquots at approximately 1:45, 4:15, 6:30, 10:15, 14:45, 19:00, 29:30 and 40:45 min (the exact collection time of each sample was recorded and used for the subsequent data analysis).

Electrophile solution 1: **1** (116 µL, 1.0 mmol), hexadecane (59 µL, 0.2 mmol) made up to 1.00 mL with toluene.

Electrophile solution 2: **1** (232 µL, 2.0 mmol), hexadecane (59 µL, 0.2 mmol) made up to 1.00 mL with toluene.

Nucleophile solution 1: **2** (103 µL, 1.0 mmol), **3** (286 µL, 1.2 mmol) made up to 1.00 mL with toluene.

Nucleophile solution 2: **2** (207 µL, 2.0 mmol), **3** (286 µL, 1.2 mmol) made up to 1.00 mL with toluene.

Nucleophile solution 3: **2** (103 µL, 1.0 mmol), **3** (572 µL, 2.0 mmol) made up to 1.00 mL with toluene.

Reaction 1. Electrophile solution 1 + nucleophile solution 1: 0.5 M **1**, 0.5 M **2**, 0.6 M **3**.

Reaction 2. Electrophile solution 2 + nucleophile solution 1: 1.0 M **1**, 0.5 M **2**, 0.6 M **3**.

Reaction 3. Electrophile solution 1 + nucleophile solution 2: 0.5 M **1**, 1.0 M **2**, 0.6 M **3**.

Reaction 4. Electrophile solution 1 + nucleophile solution 3: 0.5 M **1**, 0.5 M **2**, 1.0 M **3**.

1-Fluoro-4-nitrobenzene + morpholine. *General procedure*. Solutions of **5** with hexadecane were prepared in MeCN ("electrophile solutions"). Solutions of **6** with **7** were prepared in MeCN ("nucleophile solutions"). For each reaction, 0.5 mL of the desired electrophile solution and 0.5 mL of the desired nucleophile solution were separately loaded into two 2.5 mL Hamilton glass syringes, installed onto the Chemxy fusion 200 dual channel syringe pump, primed, and connected to the cross-mixer of the flow reactor. The reactor coils were submerged in an 80 °C water bath. The valves were not submerged but placed just above the surface of the water.

Reaction slugs were formed as in the exemplary procedure and the initial N_2 flow rate was also the same at 0.8 mL/min. Valve operation was identical. Samples were manually collected into GC vials using 600 μL of MeCN to elute from the sample loop, quenching by dilution and cooling. After the first two samples had been collected the N_2 flow was set to 0.5 mL/min, then after two more samples had been collected N_2 flow was set to 0.2 mL/min and 4 more samples were collected. This allowed collection of reaction aliquots at approximately 1:20, 3:00, 5:30, 8:15, 16:15, 25:00, 35:00 and 44:00 min (the exact collection time of each sample was recorded and used for the subsequent data analysis).

Electrophile solution 1: **5** (106 μL, 1.0 mmol), 1,3,5-trimethoxybenzene (134 mg, 0.8 mmol) made up to 1.00 mL with MeCN.

Electrophile solution 2: **5** (212 μL, 2.0 mmol), 1,3,5-trimethoxybenzene (135 mg, 0.8 mmol) made up to 1.00 mL with MeCN.

Nucleophile solution 1: **6** (87 μL, 1.0 mmol), **7** (150 μL, 1.0 mmol) made up to 1.00 mL with MeCN.

Nucleophile solution 2: **6** (174 μL, 2.0 mmol), **7** (150 μL, 1.0 mmol) made up to 1.00 mL with MeCN.

Nucleophile solution 3: **6** (87 μL, 1.0 mmol), **7** (300 μL, 2.0 mmol) made up to 1.00 mL with MeCN.

Reaction 1. Electrophile solution 1 + nucleophile solution 1: 0.5 M **5**, 0.5 M **6**, 0.5 M **7**.

Reaction 2. Electrophile solution 2 + nucleophile solution 1: 1.0 M **5**, 0.5 M **6**, 0.5 M **7**.

Reaction 3. Electrophile solution 1 + nucleophile solution 2: 0.5 M **5**, 1.0 M **6**, 0.5 M **7**.

Reaction 4. Electrophile solution 1 + nucleophile solution 3: 0.5 M **5**, 0.5 M **6**, 1.0 M **7**.

TBSCl and 2-iodobenzyl alcohol. *General procedure*. Solutions of **9** with hexadecane were prepared in DCM (electrophile solutions). Solutions of **10** with **3** and **11** were prepared in DCM (nucleophile solutions). For each reaction 0.5 mL of desired electrophile solution and 0.5 mL of desired nucleophile solution were separately loaded into two 2.5 mL Hamilton glass syringes, installed onto the Chemxy fusion 200 dual channel syringe pump and primed, then connected cross-mixer of the flow reactor. The reactor coils were submerged in an 0 °C ice-water bath. The valves were not submerged but placed just above the surface of the ice bath.

Reaction slugs were formed as in the exemplary procedure and the initial N_2 flow rate was also the same at 0.8 mL/min. Valve operation was identical. Samples were manually collected into GC vials containing 100 μL MeOH for quench using 600 μL of EtOAc to elute from the sample loop. After the first three samples had been collected the N_2 flow was set to 0.4 mL/min and an additional 5 samples were collected. This allowed collection of reaction aliquots at approximately 1:40, 3:40, 5:50, 9:40, 14:20, 18:40, 23:20 and 27:40 min (the exact collection time of each sample was recorded and used for the subsequent data analysis).

Electrophile solution 1: **9** (1.50 g, 10 mmol) and hexadecane (586 μL, 2.0 mmol) was diluted to 10.00 mL with DCM.

Electrophile solution 2: 0.55 mL of electrophile solution 1 and hexadecane (264 μL, 0.09 mmol) was diluted to 10.00 mL with DCM.

Nucleophile solution 1: **10** (116 mg, 0.50 mmol), **3** (143 μL, 0.6 mmol), **11** (6.6 μL, 0.050 mmol) made up to 0.50 mL with DCM.

Nucleophile solution 2: **10** (117 mg, 0.50 mmol), **3** (143 μL, 0.6 mmol), **11** (3.3 μL, 0.025 mmol) made up to 0.50 mL with DCM.

Nucleophile solution 3: **10** (176 mg, 0.75 mmol), **3** (143 μL, 0.6 mmol), **11** (6.6 μL, 0.05 mmol) made up to 0.50 mL with DCM.

Nucleophile solution 4: **10** (117 mg, 0.50 mmol), **3** (238 μL, 1.0 mmol), **11** (6.6 μL, 0.05 mmol) made up to 0.50 mL with DCM.

Reaction 1. Electrophile solution 1 + nucleophile solution 1: 0.28 M **9**, 0.25 M **10**, 0.3 M **3**, 0.025 M **11**.

Reaction 2. Electrophile solution 1 + nucleophile solution 2: 0.28 M **9**, 0.25 M **10**, 0.3 M **3**, 0.013 M **11**.

Reaction 3. Electrophile solution 1 + nucleophile solution 3: 0.28 M **9**, 0.38 M **10**, 0.3 M **3**, 0.025 M **11**.

Reaction 4. Electrophile solution 1 + nucleophile solution 4: 0.28 M **9**, 0.25 M **10**, 0.5 M **3**, 0.025 M **11**.

Reaction 5. Electrophile solution 2 + nucleophile solution 4: 0.5 M **9**, 0.25 M **10**, 0.5 M **3**, 0.025 M **11**.

1-Bromoethylbenzene + EtOH. *General procedure*. A 1.0 M solution of **13** was prepared in EtOH or EtOH:*t*-BuOH mixture ("electrophile solutions") and loaded into a 2.5 mL Hamilton glass syringe (no background reaction was observed at room temperature over several hours). Solutions of **15** in EtOH or EtOH:*t*-BuOH mixture were prepared and loaded into a second 2.5 mL Hamilton glass syringe. The two syringes were installed onto the Chemxy fusion 200 dual channel syringe pump, primed, and connected to the cross-mixer of the flow reactor. The reactor coils were submerged in the water bath at desired reaction temperature. The valves were placed just above the surface of the water bath.

Reaction slugs were formed as in the exemplary procedure. The initial N_2 flow rate was varied depending on the reaction temperature used and are given below for each reaction temperature. Valve operation was identical. Samples were manually collected into GC vials using 600 μL of MeCN to elute from the sample loop, quenching by dilution and cooling.

Electrophile solution 1: **13** (273 μL, 2.0 mmol), 1,3,5-trimethoxybenzene (269 mg, 1.6 mmol) made up to 2.00 mL with EtOH.

Electrophile solution 2: **13** (136 μL, 1.0 mmol), 1,3,5-trimethoxybenzene (135 mg, 0.8 mmol) made up to 1.00 mL with 4:1 EtOH:*t*-BuOH.

Electrophile solution 3: **13** (136 μL, 1.0 mmol), 1,3,5-trimethoxybenzene (137 mg, 0.8 mmol) made up to 1.00 mL with 10:1 EtOH:*t*-BuOH.

TosOH solution 1: TosOH (95 mg, 0.5 mmol) made up to 2.00 mL with EtOH.

TosOH solution 2: TosOH (96 mg, 0.5 mmol) made up to 10.00 mL with EtOH.

TosOH solution 3: TosOH (47 mg, 0.25 mmol) made up to 1.00 mL with 4:1 EtOH:*t*-BuOH.

TosOH solution 4: TosOH (46 mg, 0.25 mmol) made up to 1.00 mL with 10:1 EtOH:*t*-BuOH.

Reaction 1. Electrophile solution 1 + TosOH solution 1, 40 °C. N_2 flow 0.5 mL/min, samples collected at 3:30, 6:20, 9:30 min then N_2 flow decreased to 0.2 mL/min, samples collected at 17:45, 29:00, 40:00, 51:00 min.

Reaction 2. Electrophile solution 1 + TosOH solution 1, 50 °C. N_2 flow 0.5 mL/min, samples collected at 2:15, 5:15, 8:15, 11:15 min then N_2 flow decreased to 0.2 mL/min, samples collected at 16:20, 23:10, 29:00, 34:45, 40:20, 46:00 min.

Reaction 3. Electrophile solution 1 + TosOH solution 1, 60 °C. N_2 flow 0.6 mL/min, samples collected at 2:00, 4:15, 6:40 min then N_2 flow decreased to 0.4 mL/min, samples collected at 10:00, 14:00, 17:45 min then N_2 flow decreased to 0.3 mL/min, samples collected at 23:00, 28:30, 34:10, 39:30, 45:10 min.

Reaction 4. Electrophile solution 1 + TosOH solution 1, 70 °C. N_2 flow 0.6 mL/min, samples collected at 1:45, 4:00, 6:30 min then N_2 flow decreased to 0.4 mL/min, samples collected at 9:40, 13:30, 17:00 min then N_2 flow decreased to 0.3 mL/min, samples collected at 22:20, 27:15, 32:45, 37:45 min.

Reaction 5. Electrophile solution 1 + TosOH solution 1, 80 °C. N_2 flow 0.7 mL/min, samples collected at 1:30, 3:30, 5:30 min then N_2 flow decreased to 0.5 mL/min, samples collected at 7:45, 10:30, 13:15 min then N_2 flow decreased to 0.3 mL/min, samples collected at 18:00, 23:15, 28:15 min.

Reaction 6. Electrophile solution 1 + TosOH solution 2, 70 °C. N_2 flow 0.6 mL/min, samples collected at 1:45, 4:15, 6:50 min then N_2 flow decreased to 0.4 mL/min, samples collected at 10:30, 14:45, 19:00 min then N_2 flow decreased to 0.3 mL/min, samples collected at 24:10, 30:15, 36:30 min.

Reaction 7. Electrophile solution 2 + TosOH solution 3, 70 °C. N_2 flow 0.6 mL/min, samples collected at 1:45, 4:10, 6:35 min then N_2 flow decreased to 0.4 mL/min, samples collected at 10:00, 14:20, 18:15 min then N_2 flow decreased to 0.3 mL/min, samples collected at 23:30, 29:00, 34:30, 29:50 min.

Reaction 8. Electrophile solution 3 + TosOH solution 4, 70 °C. N_2 flow 0.6 mL/min, samples collected at 1:50, 4:15, 6:45 min then N_2 flow decreased to 0.4 mL/min, samples collected at 9:50, 14:00, 17:40 min then N_2 flow decreased to 0.3 mL/min, samples collected at 23:00, 28:20, 33:50, 39:50 min.

TBS protected 2-iodobenzyl alcohol + *t*-BuSH. *General procedure*. Solutions were prepared under Ar in oven dried glassware. A stock solution of Pd(*t*-BuXPhos)(allyl)Cl was prepared by combining $[PdCl(allyl)]_2$ and *t*-BuXPhos in THF and aging 10 min ("catalyst solution"). Solutions of **12**, **17**, **3** and hexadecane were prepared in THF ("substrate solutions"). The reactor was purged with N_2 at 0.8 mL/min for 1 h before experiments were conducted. For each reaction, 0.5 mL of desired catalyst solution and 0.5 mL of desired substrate solution were separately loaded into two 2.5 mL Hamilton glass syringes, installed onto the Chemxy fusion 200 dual channel syringe pump, primed, and connected to the cross-mixer of the flow reactor.

Reaction slugs were formed as in the exemplary procedure and the initial N_2 flow rate was the same at 0.8 mL/min. Valve operation was identical. Samples were manually collected into GC vials using 600 μL of EtOAc to elute from the sample loop, quenching by dilution. Five samples were collected at approximately 1:30, 3:25, 5:25, 7:20 and 9:10 min (the exact collection time of each sample was recorded and used for the subsequent data analysis).

Order in catalyst experiments:

Catalyst solution 1: $[PdCl(allyl)]_2$ (5.7 mg, 0.016 mmol) and *t*-BuXPhos (3.6 mg, 0.032 mmol) were made up to 4.00 mL with THF.

Catalyst solution 2: 0.75 mL of catalyst solution 1 was diluted to 1.00 mL with THF.

Catalyst solution 3: 0.50 mL of catalyst solution 1 was diluted to 1.00 mL with THF.

Catalyst solution 4: 0.50 mL of catalyst solution 1 was diluted to 2.00 mL with THF.

Catalyst solution 5: 0.50 mL of catalyst solution 4 was diluted to 1.00 mL with THF.

Substrate solution 1: **12** (52 μL, 70 mg, 0.2 mmol), **17** (34 μL, 0.3 mmol), **3** (95 μL, 0.4 mmol), hexadecane (58 μL, 0.2 mmol) made up to 2.00 mL with THF.

Reaction 1. Catalyst solution 2 + substrate solution 1: 0.05 M **12**, 0.075 M **17**, 0.1 M **3**, 0.003 M Pd(*t*-BuXPhos)(allyl)Cl (6%).

Reaction 2. Catalyst solution 3 + substrate solution 1: 0.05 M **12**, 0.075 M **17**, 0.1 M **3**, 0.002 M Pd(*t*-BuXPhos)(allyl)Cl (4%).

Reaction 3. Catalyst solution 4 + substrate solution 1: 0.05 M **12**, 0.075 M **17**, 0.1 M **3**, 0.001 M Pd(*t*-BuXPhos)(allyl)Cl (2%).

Reaction 4. Catalyst solution 5 + substrate solution 1: 0.05 M **12**, 0.075 M **17**, 0.1 M **3**, 0.0005 M Pd(*t*-BuXPhos)(allyl)Cl (1%).

Order in ArI experiments:

Catalyst solution 1: $[PdCl(allyl)]_2$ (4.3 mg, 0.012 mmol) and *t*-BuXPhos (10.1 mg, 0.024 mmol) were made up to 4.00 mL with THF.

Substrate solution 1: **12** (39 μL, 52 mg, 0.15 mmol), **17** (8.4 μL, 0.075 mmol), **3** (24 μL, 0.1 mmol), hexadecane (15 μL, 0.05 mmol) made up to 0.50 mL with THF.

Substrate solution 2: **12** (26 μL, 35 mg, 0.1 mmol), **17** (8.4 μL, 0.075 mmol), **3** (24 μL, 0.1 mmol), hexadecane (15 μL, 0.05 mmol) made up to 0.50 mL with THF.

Substrate solution 3: **12** (13 μL, 17 mg, 0.05 mmol), **17** (8.4 μL, 0.075 mmol), **3** (24 μL, 0.1 mmol), hexadecane (15 μL, 0.05 mmol) made up to 0.50 mL with THF.

Substrate solution 4: **12** (6.5 μL, 9 mg, 0.025 mmol), **17** (8.4 μL, 0.075 mmol), **3** (24 μL, 0.1 mmol), hexadecane (15 μL, 0.05 mmol) made up to 0.50 mL with THF.

Substrate solution 5: **12** (3.2 μL, 4 mg, 0.013 mmol), **17** (8.4 μL, 0.075 mmol), **3** (24 μL, 0.1 mmol), hexadecane (15 μL, 0.05 mmol) made up to 0.50 mL with THF.

Reaction 1. Catalyst solution 1 + substrate solution 1: 0.15 M **12**, 0.075 M **17**, 0.1 M **3**, 0.003 M Pd(*t*-BuXPhos)(allyl)Cl.

Reaction 2. Catalyst solution 1 + substrate solution 2: 0.1 M **12**, 0.075 M **17**, 0.1 M **3**, 0.003 M Pd(*t*-BuXPhos)(allyl)Cl.

Reaction 3. Catalyst solution 1 + substrate solution 3: 0.05 M **12**, 0.075 M **17**, 0.1 M **3**, 0.003 M Pd(*t*-BuXPhos)(allyl)Cl.

Reaction 4. Catalyst solution 1 + substrate solution 4: 0.025 M **12**, 0.075 M **17**, 0.1 M **3**, 0.003 M Pd(*t*-BuXPhos)(allyl)Cl.

Reaction 5. Catalyst solution 1 + substrate solution 5: 0.013 M **12**, 0.075 M **17**, 0.1 M **3**, 0.003 M Pd(*t*-BuXPhos)(allyl)Cl.

Order in *t*-BuSH experiments:

Catalyst solution 1: $[PdCl(allyl)]_2$ (4.3 mg, 0.012 mmol) and *t*-BuXPhos (10.2 mg, 0.024 mmol) were made up to 4.00 mL with THF.

Substrate solution 1: **12** (13 μL, 17 mg, 0.05 mmol), **17** (34 μL, 0.3 mmol), **3** (24 μL, 0.1 mmol), hexadecane (15 μL, 0.05 mmol) made up to 0.50 mL with THF.

Substrate solution 2: **12** (13 μL, 17 mg, 0.05 mmol), **17** (17 μL, 0.15 mmol), **3** (24 μL, 0.1 mmol), hexadecane (15 μL, 0.05 mmol) made up to 0.50 mL with THF.

Substrate solution 3: **12** (13 μL, 17 mg, 0.05 mmol), **17** (8.4 μL, 0.075 mmol), **3** (24 μL, 0.1 mmol), hexadecane (15 μL, 0.05 mmol) made up to 0.50 mL with THF.

Substrate solution 4: **12** (13 μL, 17 mg, 0.05 mmol), **17** (4.2 μL, 0.038 mmol), **3** (24 μL, 0.1 mmol), hexadecane (15 μL, 0.05 mmol) made up to 0.50 mL with THF.

Substrate solution 5: **12** (13 μL, 17 mg, 0.05 mmol), **17** (2.1 μL, 0.019 mmol), **3** (24 μL, 0.1 mmol), hexadecane (15 μL, 0.05 mmol) made up to 0.50 mL with THF.

Substrate solution 6: **12** (13 μL, 17 mg, 0.05 mmol), **17** (1.0 μL, 0.0094 mmol), **3** (24 μL, 0.1 mmol), hexadecane (15 μL, 0.05 mmol) made up to 0.50 mL with THF.

Reaction 1. Catalyst solution 1 + substrate solution 1: 0.05 M **12**, 0.3 M **17**, 0.1 M **3**, 0.003 M Pd(*t*-BuXPhos)(allyl)Cl.

Reaction 2. Catalyst solution 1 + substrate solution 2: 0.05 M **12**, 0.15 M **17**, 0.1 M **3**, 0.003 M Pd(*t*-BuXPhos)(allyl)Cl.

Reaction 3. Catalyst solution 1 + substrate solution 3: 0.05 M **12**, 0.075 M **17**, 0.1 M **3**, 0.003 M Pd(*t*-BuXPhos)(allyl)Cl.

Reaction 4. Catalyst solution 1 + substrate solution 4: 0.05 M **12**, 0.038 M **17**, 0.1 M **3**, 0.003 M Pd(*t*-BuXPhos)(allyl)Cl.

Reaction 5. Catalyst solution 1 + substrate solution 5: 0.05 M **12**, 0.019 M **17**, 0.1 M **3**, 0.003 M Pd(*t*-BuXPhos)(allyl)Cl.

Reaction 6. Catalyst solution 1 + substrate solution 6: 0.05 M **12**, 0.0094 M **17**, 0.1 M **3**, 0.003 M Pd(*t*-BuXPhos)(allyl)Cl.

Order in Bu_3N experiments:

Catalyst solution 1: $[PdCl(allyl)]_2$ (4.2 mg, 0.012 mmol) and *t*-BuXPhos (10.0 mg, 0.024 mmol) were made up to 4.00 mL with THF.

Substrate solution 1: **12** (13 μL, 17 mg, 0.05 mmol), **17** (8.4 μL, 0.075 mmol), **3** (36 μL, 0.15 mmol), hexadecane (15 μL, 0.05 mmol) made up to 0.50 mL with THF.

Substrate solution 2: **12** (13 μL, 17 mg, 0.05 mmol), **17** (8.4 μL, 0.075 mmol), **3** (24 μL, 0.1 mmol), hexadecane (15 μL, 0.05 mmol) made up to 0.50 mL with THF.

Substrate solution 3: **12** (13 μL, 17 mg, 0.05 mmol), **17** (8.4 μL, 0.075 mmol), **3** (12 μL, 0.05 mmol), hexadecane (15 μL, 0.05 mmol) made up to 0.50 mL with THF.

Substrate solution 4: **12** (13 μL, 17 mg, 0.05 mmol), **17** (8.4 μL, 0.075 mmol), **3** (6 μL, 0.025 mmol), hexadecane (15 μL, 0.05 mmol) made up to 0.50 mL with THF.

Substrate solution 5: **12** (13 μL, 17 mg, 0.05 mmol), **17** (8.4 μL, 0.075 mmol), **3** (3 μL, 0.013 mmol), hexadecane (15 μL, 0.05 mmol) made up to 0.50 mL with THF.

Reaction 1. Catalyst solution 1 + substrate solution 1: 0.05 M **12**, 0.075 M **17**, 0.15 M **3**, 0.003 M Pd(*t*-BuXPhos)(allyl)Cl.

Reaction 2. Catalyst solution 1 + substrate solution 2: 0.05 M **12**, 0.075 M **17**, 0.1 M **3**, 0.003 M Pd(*t*-BuXPhos)(allyl)Cl.

Reaction 3. Catalyst solution 1 + substrate solution 3: 0.05 M **12**, 0.075 M **17**, 0.05 M **3**, 0.003 M Pd(*t*-BuXPhos)(allyl)Cl.

Reaction 4. Catalyst solution 1 + substrate solution 4: 0.05 M **12**, 0.075 M **17**, 0.025 M **3**, 0.003 M Pd(*t*-BuXPhos)(allyl)Cl.

Reaction 5. Catalyst solution 1 + substrate solution 5: 0.05 M **12**, 0.075 M **17**, 0.013 M **3**, 0.003 M Pd(*t*-BuXPhos)(allyl)Cl.

Cyclopentadiene + methyl acrylate. Solutions of **21** with hexadecane were prepared in $CHCl_3$ ("acrylate solutions"). A 2.25 M solution of **20** in $CHCl_3$ was prepared by diluting freshly distilled **20** (189 μL, 2.25 mmol) up to 1.00 mL with $CHCl_3$ ("diene solution").

Acrylate solution 1: **21** (34 μL, 0.38 mmol), hexadecane (22 μL, 0.075 mmol) up to 0.50 mL with $CHCl_3$.

Acrylate solution 2: **21** (68 μL, 0.75 mmol), hexadecane (22 μL, 0.075 mmol) up to 0.50 mL with $CHCl_3$.

Acrylate solution 3: **21** (68 μL, 0.75 mmol), hexadecane (44 μL, 0.15 mmol) up to 0.50 mL with $CHCl_3$.

Slugs were loaded into the loading coil by taking the desired acrylate solution into a 2.5 mL Hamilton glass syringe, installing on the Fusion 200 syringe pump, priming and then connecting to the first tee-mixer (see Figure S8 in the supporting information). The slugs were loaded as follows: 333 μL of acrylate solution 1, 150 μL of H_2O, 333 μL of acrylate solution 2, 150 μL of H_2O, 167 μL of acrylate solution 3, 50 μL of H_2O.

The diene solution was then loaded into a 2.5 mL Hamilton glass syringe, installed on the Fusion 200 syringe pump and primed. The syringe was then connected to the second tee-mixer (see Figure S9 in the supporting information) and 50 μL was eluted to prime the tubing.

Reactor valves were set to the following positions: Valve 1, position 1; valve 2, position 1; sampling valve set to collect sample and the reactor coils were lowered into a 70 °C water bath.

The SyrDos pump was started at 200 μL/min until the dienophile solution 1 slug approached the second tee-mixer. The SyrDos flow rate was then decreased to 133 μL/min and the diene solution was delivered at 67 μL/min to give a 0.5 mL reaction slug 0.5 M in **21** and 0.75 M in **20**. After the dienophile solution 1 slug completely exited the loading coil the SyrDos flow rate was set to 200 μL/min again and the diene pump was stopped.

Once the dienophile solution 2 slug approached the second tee-mixer the SyrDos flow rate was again set to 133 μL/min and the diene solution was delivered at a rate of 67 μL/min, initiating the second 0.5 mL reaction slug that was 1.0 M in **21**

and 0.75 M in **20**. After the dienophile solution 2 slug completely exited the loading coil the SyrDos flow rate was set back to 200 μL/min again and the diene pump was stopped.

As the last slug (dienophile solution 3) approached the second tee-mixer, the SyrDos flow rate was decreased to 67 μL/min and the diene solution was delivered at 133 μL/min, initiating the last 0.5 mL reaction plug that was 0.5 M in **21** and 1.5 M in **20**. After the dienophile solution 3 slug completely exited the loading coil the SyrDos pump was set to 200 μL/min again and the diene solution pump was stopped.

All three reaction plugs were now formed and travelling inside coil A. Once the first reaction slug entered the sampling valve, and ~50 μL had passed through, the sampling valve was actuated and a 15 μL aliquot sample was eluted with 600 μL EtOAc into a GC vial. The sample removal line was then flushed with H_2O. Once the remainder of the reaction slug had exited the sampling valve, the sampling valve was set back to the position to collect a new sample, and the sample removal line was then flushed with EtOAc.

Once the second reaction slug entered the sampling valve, and ~50 μL had passed through, the sampling valve was again actuated and a 15 μL aliquot sample was eluted with 600 μL EtOAc into a GC vial. The sample removal line was then flushed with H_2O. Once the remainder of the reaction slug had exited the sampling valve, the sampling valve was set back to the position to collect a new sample, and the sample removal line was then flushed with EtOAc.

Once the third reaction slug entered the sampling valve, and ~50 μL had passed through, the sampling valve was again actuated and a 15 μL aliquot sample was eluted with 600 μL EtOAc into a GC vial. The sample removal line was then flushed with H_2O. Once the remainder of the reaction slug had exited the sampling valve, and fully passed through valve 1 to coil B, valve 1 was set to position 2, valve 2 was set to position 2 (clockwise rotation) and the sampling valve was set to collect a sample again.

All three reaction slugs were now travelling through coil B. Sampling was continued in the same manner as each reaction plug again passed through the sampling valve. After all three reaction slugs had passed back into coil A, the reactor valves were again actuated: valve 1 to position 1, valve 2 to position 1 (counter-clockwise rotation), and the sampling valve to collection. Sampling and valve actuation were repeated to collect desired samples.

Note. In experiments using N_2 as the carrier fluid the entire reaction slug was formed very quickly (~5 s) to facilitate the ability to increase the sample interval as the reaction progressed by decreasing the N_2 flow rate without needing to consider residence time discrepancies between the front and back of the reaction slug. In these experiments however, the use of residence time was necessary to facilitate multiple consecutive reaction slugs and therefore reactions were initiated at the same flow rate as the carrier flow rate for the entire reaction progress. In order to increase the interval between sample collection as the reaction progressed therefore the carrier flow rate was unchanged and sample collection was simply skipped at 50, 1:10, 1:30, 1:50, 2:10, 2:20, 2:40 and 2:50 min. To skip sample collection, the sampling valve was simply not actuated as the reaction slugs travelled through, and only reactor valves 1 and 2 were actuated after all three reaction slugs had passed from one reactor coil into the other.

ASSOCIATED CONTENT

Supporting Information. Details of the flow reactor and equipment, comparison batch kinetic data, flow kinetic data used for determination of reaction orders, calculated reaction pathway for the C-S cross-coupling, troubleshooting and limitations, calibration curves, computational details. This material is available free of charge via the Internet at http://pubs.acs.org.

AUTHOR INFORMATION

Corresponding Author

* *stephen.newman@uottawa.ca*

ORCID

Ryan J. Sullivan: 0000-0001-5540-6962
Stephen G. Newman: 0000-0003-1949-5069

Notes

The authors declare no competing financial interest.

ACKNOWLEDGMENTS

Financial support for this work was provided by the University of Ottawa, the National Science and Engineering Research Council of Canada (NSERC), and the Canada Research Chair program. The Canadian Foundation for Innovation (CFI) and the Ontario Ministry of Economic Development and Innovation are thanked for essential infrastructure. Debasis Mallik (CCRI flow chemistry facility) and Peter Zhang (Vici Valco) are thanked for programming the drivers used to control the sampling valves. R. J. S. thanks NSERC for a CGS-D award.

REFERENCES

(1) (a) Moore, J. W.; Pearson, R. G. *Kinetics and Mechanism*; 3 ed.; Wiley: New York, 1981; (b) Masel, R. I. *Chemical Kinetics and Catalysis*; Wiley: New York, 2001; (c) Blackmond, D. G. Reaction Progress Kinetic Analysis: A Powerful Methodology for Mechanistic Studies of Complex Catalytic Reactions. *Angew. Chem. Int. Ed.* **2005**, *44*, 4302–4320; (d) Blackmond, D. G. Kinetic Profiling of Catalytic Organic Reactions as a Mechanistic Tool. *J. Am. Chem. Soc.* **2015**, *137*, 10852–10866.

(2) (a) Fermier, A. M.; Oyler, A. R.; Armstrong, B. L.; Weber, B. A.; Rodriguez, R. L.; Weber, J. V.; Nalasco, J. A. Automation of Chemical Reaction Kinetics and Product Distribution Studies in Pharmaceutical Development. *J. Assoc. Lab. Automation* **2002**, *7*, 83–88; (b) Chung, R.; Yu, D.; Thai, V. T.; Jones, A. F.; Veits, G. K.; Read de Alaniz, J.; Hein, J. E. Tandem Reaction Progress Analysis as a Means for Dissecting Catalytic Reactions: Application to the Aza-Piancatelli Rearrangement. *ACS Catal.* **2015**, *5*, 4579–4585; (c) Rougeot, C.; Situ, H.; Cao, B. H.; Vlachos, V.; Hein, J. E. Automated Reaction Progress Monitoring of Heterogeneous Reactions: Crystallization-Induced Stereoselectivity in Amine-Catalyzed Aldol Reactions. *React. Chem. Eng.* **2017**, *2*, 226–231; (d) Malig, T. C.; Koenig, J. D. B.; Situ, H.; Chehal, N. K.; Hultin, P. G.; Hein, J. E. Real-Time HPLC-MS Reaction Progress Monitoring Using an Automated Analytical Platform. *React. Chem. Eng.* **2017**, *2*, 309–314; (e) Fermier, A. M.; Oyler, A. R.; Armstrong, B. L.; Weber, J. V.; Nalasco, J. Apparatus for the Automation of Chemical Reaction Kinetics Studies. WO patent WO2002/077614 A2, 2002.

(3) (a) Burés, J. A Simple Graphical Method to Determine the Order in Catalyst. *Angew. Chem. Int. Ed.* **2016**, *55*, 2028–2031; (b) Burés, J. Variable Time Normalization Analysis: General Graphical Elucidation of Reaction Orders from Concentration Profiles. *Angew. Chem. Int. Ed.* **2016**, *55*, 16084–16087; (c) Martínez-Carrión, A.; Howlett, M. G.; Alamillo-Ferrer, C.; Clayton, A. D.; Bourne, R. A.; Codina, A.; Vidal-Ferran, A.; Adams, R. W.; Burés, J. Kinetic Treatments for Catalyst Activation and Deactivation Processes based on Variable Time

Normalization Analysis. *Angew. Chem. Int. Ed.* **2019**, *58*, 10189–10193.

(4) (a) McMullen, J. P.; Jensen, K. F. Integrated Microreactors for Reaction Automation: New Approaches to Reaction Development. *Annu. Rev. Anal. Chem.* **2010**, *3*, 19–42; (b) Hartman, R. L.; McMullen, J. P.; Jensen, K. F. Deciding Whether To Go with the Flow: Evaluating the Merits of Flow Reactors for Synthesis. *Angew. Chem. Int. Ed.* **2011**, *50*, 7502–7519; (c) Newman, S. G.; Jensen, K. F. The Role of Flow in Green Chemistry and Engineering. *Green Chem.* **2013**, *15*, 1456–1472; (d) Ley, S. V.; Fitzpatrick, D. E.; Ingham, R. J.; Myers, R. M. Organic Synthesis: March of the Machines. *Angew. Chem. Int. Ed.* **2015**, *54*, 3449–3464.

(5) Valera, F. E.; Quaranta, M.; Moran, A.; Blacker, J.; Armstrong, A.; Cabral, J. T.; Blackmond, D. G. The Flow's the Thing…□Or Is It? Assessing the Merits of Homogeneous Reactions in Flask and Flow. *Angew. Chem. Int. Ed.* **2010**, *49*, 2478–2485.

(6) For example: (a) McMullen, J. P.; Jensen, K. F. Rapid Determination of Reaction Kinetics with an Automated Microfluidic System. *Org. Process Res. Dev.* **2011**, *15*, 398–407; (b) Gholamipour-Shirazi, A.; Rolando, C. Alkylation of Substituted Benzoic Acids in a Continuous Flow Microfluidic Microreactor: Kinetics and Linear Free Energy Relationships. *Org. Process Res. Dev.* **2012**, *16*, 811–818; (c) Roberge, D. M.; Noti, C.; Irle, E.; Eyholzer, M.; Rittiner, B.; Penn, G.; Sedelmeier, G.; Schenkel, B. Control of Hazardous Processes in Flow: Synthesis of 2-Nitroethanol. *J. Flow Chem.* **2014**, *4*, 26–34; (d) Hone, C. A.; Boyd, A.; O'Kearney-McMullan, A.; Bourne, R. A.; Muller, F. L. Definitive Screening Designs for Multistep Kinetic Models in Flow. *React. Chem. Eng.* **2019**, *4*, 1565–1570.

(7) (a) Mozharov, S.; Nordon, A.; Littlejohn, D.; Wiles, C.; Watts, P.; Dallin, P.; Girkin, J. M. Improved Method for Kinetic Studies in Microreactors Using Flow Manipulation and Noninvasive Raman Spectrometry. *J. Am. Chem. Soc.* **2011**, *133*, 3601–3608; (b) Moore, J. S.; Jensen, K. F. "Batch" Kinetics in Flow: Online IR Analysis and Continuous Control. *Angew. Chem. Int. Ed.* **2014**, *53*, 470–473; (c) Schwolow, S.; Braun, F.; Rädle, M.; Kockmann, N.; Röder, T. Fast and Efficient Acquisition of Kinetic Data in Microreactors Using In-Line Raman Analysis. *Org. Process Res. Dev.* **2015**, *19*, 1286–1292; (d) Durand, T.; Henry, C.; Bolien, D.; Harrowven, D. C.; Bloodworth, S.; Franck, X.; Whitby, R. J. Thermolysis of 1,3-dioxin-4-ones: fast generation of kinetic data using in-line analysis under flow. *React. Chem. Eng.* **2016**, *1*, 82–89; (e) Hone, C. A.; Holmes, N.; Akien, G. R.; Bourne, R. A.; Muller, F. L. Rapid Multistep Kinetic Model Generation From Transient Flow Data. *React. Chem. Eng.* **2017**, *2*, 103–108; (f) Aroh, K. C.; Jensen, K. F. Efficient Kinetic Experiments in Continuous Flow Microreactors. *React. Chem. Eng.* **2018**, *3*, 94–101.

(8) (a) Reizman, B. J.; Jensen, K. F. Feedback in Flow for Accelerated Reaction Development. *Acc. Chem. Res.* **2016**, *49*, 1786–1796; (b) Mascia, S.; Heider, P. L.; Zhang, H.; Lakerveld, R.; Benyahia, B.; Barton, P. I.; Braatz, R. D.; Cooney, C. L.; Evans, J. M. B.; Jamison, T. F.; Jensen, K. F.; Myerson, A. S.; Trout, B. L. End-to-End Continuous Manufacturing of Pharmaceuticals: Integrated Synthesis, Purification, and Final Dosage Formation. *Angew. Chem. Int. Ed.* **2013**, *52*, 12359–12363; (c) Adamo, A.; Beingessner, R. L.; Behnam, M.; Chen, J.; Jamison, T. F.; Jensen, K. F.; Monbaliu, J.-C. M.; Myerson, A. S.; Revalor, E. M.; Snead, D. R.; Stelzer, T.; Weeranoppanant, N.; Wong, S. Y.; Zhang, P. On-Demand Continuous-Flow Production of Pharmaceuticals in a Compact, Reconfigurable System. *Science* **2016**, *352*, 61–67; (d) Perera, D.; Tucker, J. W.; Brahmbhatt, S.; Helal, C. J.; Chong, A.; Farrell, W.; Richardson, P.; Sach, N. W. A Platform for Automated Nanomole-Scale Reaction Screening and Micromole-Scale Synthesis in Flow. *Science* **2018**, *359*, 429–434; (e) Coley, C. W.; Thomas, D. A.; Lummiss, J. A. M.; Jaworski, J. N.; Breen, C. P.; Schultz, V.; Hart, T.; Fishman, J. S.; Rogers, L.; Gao, H.; Hicklin, R. W.; Plehiers, P. P.; Byington, J.; Piotti, J. S.; Green, W. H.; Hart, A. J.; Jamison, T. F.; Jensen, K. F. A Robotic Platform for Flow Synthesis of Organic Compounds Informed by AI Planning. *Science* **2019**, *365*, eaax1566.

(9) (a) Plutschack, M. B.; Pieber, B.; Gilmore, K.; Seeberger, P. H. The Hitchhiker's Guide to Flow Chemistry. *Chem. Rev.* **2017**, *117*, 11796–11893; (b) Pastre, J. C.; Browne, D. L.; Ley, S. V. Flow Chemistry Syntheses of Natural Products. *Chem. Soc. Rev.* **2013**, *42*, 8849–8869; (c) Newton, S.; Carter, C. F.; Pearson, C. M.; Alves, L. D.; Lange, H.; Thansandote, P.; Ley, S. V. Accelerating Spirocyclic Polyketide Synthesis using Flow Chemistry. *Angew. Chem. Int. Ed.* **2014**, *53*, 4915–4920; (d) Cole, K. P.; Groh, J. M.; Johnson, M. D.; Burcham, C. L.; Campbell, B. M.; Diseroad, W. D.; Heller, M. R.; Howell, J. R.; Kallman, N. J.; Koenig, T. M.; May, S. A.; Miller, R. D.; Mitchell, D.; Myers, D. P.; Myers, S. S.; Phillips, J. L.; Polster, C. S.; White, T. D.; Cashman, J.; Hurley, D.; Moylan, R.; Sheehan, P.; Spencer, R. D.; Desmond, K.; Desmond, P.; Gowran, O. Kilogram-Scale Prexasertib Monolactate Monohydrate Synthesis Under Continuous-Flow CGMP Conditions. *Science* **2017**, *356*, 1144–1150; (e) K. Kashani, S.; Sullivan, R. J.; Andersen, M.; Newman, S. G. Overcoming Solid Handling Issues in Continuous Flow Substitution Reactions Through Ionic Liquid Formation. *Green Chem.* **2018**, *20*, 1748–1753; (f) Russell, M. G.; Jamison, T. F. Seven-Step Continuous Flow Synthesis of Linezolid Without Intermediate Purification. *Angew. Chem. Int. Ed.* **2019**, *58*, 7678–7681.

(10) (a) Vural Gursel, I.; Noel, T.; Wang, Q.; Hessel, V. Separation/Recycling Methods for Homogeneous Transition Metal Catalysts in Continuous Flow. *Green Chem.* **2015**, *17*, 2012–2026; (b) Sullivan, R. J.; Newman, S. G. Chiral Auxiliary Recycling in Continuous Flow: Automated Recovery and Reuse of Oppolzer's Sultam. *Chem. Sci.* **2018**, *9*, 2130–2134.

(11) For examples of reactions performed in discrete slugs or droplets see: (a) Song, H.; Chen, D. L.; Ismagilov, R. F. Reactions in Droplets in Microfluidic Channels. *Angew. Chem. Int. Ed.* **2006**, *45*, 7336–7356; (b) Sesen, M.; Alan, T.; Neild, A. Droplet Control Technologies for Microfluidic High Throughput Screening (μHTS). *Lab Chip* **2017**, *17*, 2372–2394; (c) Kaminski, T. S.; Garstecki, P. Controlled Droplet Microfluidic Systems for Multistep Chemical and Biological Assays. *Chem. Soc. Rev.* **2017**, *46*, 6210–6226; (d) Isbrandt, E. S.; Sullivan, R. J.; Newman, S. G. High Throughput Strategies for the Discovery and Optimization of Catalytic Reactions. *Angew. Chem. Int. Ed.* **2019**, *58*, 7180–7191; (f) Candoni, N.; Grossier, R.; Lagaize, M.; Veesler, S. Advances in the Use of Microfluidics to Study Crystallization Fundamentals. *Annu. Rev. Chem. Biomol.* **2019**, *10*, 59–83; (g) Hwang, Y.-J.; Coley, C. W.; Abolhasani, M.; Marzinzik, A. L.; Koch, G.; Spanka, C.; Lehmann, H.; Jensen, K. F. A Segmented Fflow Platform for On-Demand Medicinal Chemistry and Compound Synthesis in Oscillating Droplets. *Chem. Commun.* **2017**, *53*, 6649–6652.

(12) An initial version of this work was deposited in ChemRxiv on Oct 21, 2019, Sullivan, R. J.; Newman, S. G. Reaction Cycling for Efficient Kinetic Analysis in Flow. ChemRxiv **2019**. Preprint. https://doi.org/10.26434/chemrxiv.10009013.v1.

(13) Only 7 ports and 6 positions are needed. Any selector valve with ≥7-ports, 6-positions can be substituted by fabrication of a suitable rotor. See Figure S4 in the supporting information.

(14) A custom rotor for the selector valve was purchased from Vici Valco (~$100 USD).

(15) Price, G. A.; Mallik, D.; Organ, M. G. Process Analytical Tools for Flow Analysis: A Perspective. *J. Flow Chem.* **2017**, *7*, 82–86.

(16) (a) Zheng, B.; Ismagilov, R. F. A Microfluidic Approach for Screening Submicroliter Volumes against Multiple Reagents by Using Preformed Arrays of Nanoliter Plugs in a Three-Phase Liquid/Liquid/Gas Flow. *Angew. Chem. Int. Ed.* **2005**, *44*, 2520–2523; (b) Chen, D. L.; Ismagilov, R. F. Microfluidic Cartridges Preloaded with Nanoliter Plugs of Reagents: An Alternative to 96-Well Plates for Screening. *Curr. Opin. Chem. Biol.* **2006**, *10*, 226–231.

(17) Extremely fast reactions are ideally suited for traditional steady state flow kinetics experiments, since the time inefficiencies of that strategy are not problematic when investigating reactions with incredibly short timescales, and therefore we believe these are best considered complimentary tools.

(18) Reaction slugs used were 300 μL (≈ 1.5 m long in the 0.5 mm ID reactor coils) and were sampled from the center of the slug, such that concerns over solvent loss to the gaseous carrier phase or reaction acceleration at droplet interfaces were not relevant.

(19) (a) Hubbard, P.; Brittain, W. J. Mechanism of Amine-Catalyzed Ester Formation from an Acid Chloride and Alcohol. *J. Org. Chem.* **1998**, *63*, 677–683; (b) Oosthoek-de Vries, A. J.; Nieuwland, P. J.; Bart, J.; Koch, K.; Janssen, J. W. G.; van Bentum, P. J. M.; Rutjes, F. P. J. T.; Gardeniers, H. J. G. E.; Kentgens, A. P. M. Inline Reaction Monitoring of Amine-Catalyzed Acetylation of Benzyl Alcohol Using a Microfluidic Stripline Nuclear Magnetic Resonance Setup. *J. Am. Chem. Soc.* **2019**, *141*, 5369–5380.

(20) Patschinski, P.; Zhang, C.; Zipse, H. The Lewis Base-Catalyzed Silylation of Alcohols—A Mechanistic Analysis. *J. Org. Chem.* **2014**, *79*, 8348–8357.

(21) For a discussion of typical values for activation enthalpies and entropies see: Anslyn, E. V.; Dougherty, D. A. *Modern Physical Organic Chemistry*; University Science: Sausalito, 2006.

(22) Xu, J.; Liu, R. Y.; Yeung, C. S.; Buchwald, S. L. Monophosphine Ligands Promote Pd-Catalyzed C–S Cross-Coupling Reactions at Room Temperature with Soluble Bases. *ACS Catal.* **2019**, *9*, 6461–6466.

(23) When using sequential droplets in microfluidic screening platforms it is sometimes necessary to include "blank" droplets between reactions to prevent bleed through of materials (for an example see ref 11f). This was found to be unnecessary in this case, likely because this reactor uses large reaction slugs (450 μL ≈ 60 cm long slugs in the 1.0 mm ID reactor coils) rather that droplets making small amounts of bleed through inconsequential. For further information about the situations that lead to bleed through between slugs see: (a) Sebastian Cabeza, V.; Kuhn, S.; Kulkarni, A. A.; Jensen, K. F. Size-Controlled Flow Synthesis of Gold Nanoparticles Using a Segmented Flow Microfluidic Platform. *Langmuir* **2012**, *28*, 7007–7013; (b) Lee, S.; Park, J.-S.; Lee, T. R. The Wettability of Fluoropolymer Surfaces: Influence of Surface Dipoles. *Langmuir* **2008**, *24*, 4817–4826.

(24) Obtaining kinetic data from (near-)refluxing solutions in batch is hampered by unknown partitioning of volatile components (e.g., cyclopentadiene) between the reaction solution and headspace (see ref 4b) while sampling from batch vessels under pressure requires specialized autoclaves equipped with dip tubes for sample removal. In flow however, the combination of back pressure to prevent solvent boiling and no headspace facilitates collection of high-quality kinetic data above the atmospheric boiling point of reaction components.

(25) Feng, J.; Liang, S.; Chen, S.-Y.; Zhang, J.; Fu, S.-S.; Yu, X.-Q. A Metal-Free Oxidative Esterification of the Benzyl C-H Bond. *Adv. Synth. Catal.* 2012, **354**, 1287–1292.

(26) Meng, D.; Li, D.; Ollevier, T. Recyclable Iron(II) Caffeine-Derived Ionic Salt Catalyst in the Diels–Alder Reaction of Cyclopentadiene and α,β-Unsaturated N-Acyl-oxazolidinones in Dimethyl Carbonate. *RSC Advances* 2019, **9**, 21956–21963.

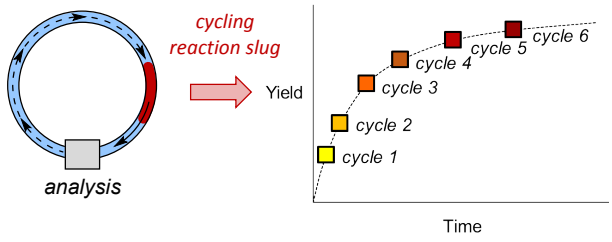
cycling
reaction slug
analysis
Yield
cycle 1
cycle 2
cycle 3
cycle 4
cycle 5
cycle 6
Time